The 11th Canadian Conference on Earthquake Engineering
Canadian Association for Earthquake Engineering
11CCEE

SEISMIC BEHAVIOUR OF EXTERIOR GFRP-RC BEAM-COLUMN JOINTS: EXPERIMENTAL AND ANALYTICAL STUDY

Shervin K.Ghomi[1] and Ehab El-Salakawy[2]
[1] Ph.D. Student, Dept. of Civil Eng., University of Manitoba, Winnipeg, MB, Canada
[2] Professor and CRC, Dept. of Civil Eng., University of Manitoba, Winnipeg, MB, Canada

ABSTRACT: Two full-scale specimens were constructed and tested under reversal cyclic loading to study the seismic behaviour of exterior GFRP-reinforced concrete (RC) beam-column joints with lateral beams. The test variable was joint shear stresses (0.85 and $1.1\sqrt{f'_c}$). The specimens were isolated from assumed points of contra-flexure at mid-height of the columns and mid-span of the beams. Test results indicated that well-designed exterior GFRP-RC beam-column joints confined with lateral beams exhibit linear behaviour with minimum residual damage up to 6% drift ratio, which is significantly higher than the maximum lateral drift ratio expected by CSA S806-12 (4%). This feature is beneficial to minimize the repairing cost of structural elements after an earthquake. In addition to the experimental study, a specialized software was used to construct a Finite Elements Model, which was verified against the test results. The verified model was used to further investigate the effect of various parameters on the joints behaviour, such as: joint shear stress, presence of lateral beams and concrete strength. Results of the analytical study indicated that the effect of lateral beams depends on the magnitude of the joint shear stress. Moreover, it was found that concrete compressive strength have significant effect on the drift ratio that beam-column joints achieve their design capacity at.

1. Introduction

In the past two decades, Fiber Reinforced Polymers (FRPs) have emerged as an alternative for steel bars and stirrups in reinforced concrete (RC) structures due to their superior behaviour in terms of corrosion resistance, electrical and magnetic non-conductivity, and high strength-to-weight ratio. Up to date, many researchers have been involved in investigating the behaviour of various FRP-RC elements. Majority of these studies focused on the behaviour of individual elements, such as beams and slabs, under monotonic loading. In contrary, studies to investigate integral behaviour of FRP-RC structures, when two or more structural elements interact with each other (such as beam-column joints and slab-column connections), are very limited (*Fukuyama et al.* 1995, *Said and Nehdi* 2004, *Mady et al.* 2011).

One of the main concerns about FRP-RC structures is their performance under earthquake-induced loads. The FRP materials exhibit linear-elastic stress-strain relationship up to failure (no yielding). This could cause brittle failure of elements and low energy dissipation of frames. In order to evaluate the seismic performance of FRP-RC frames, understanding the behaviour of beam-column joints, as a key element in stability of frames, under lateral loading is essential.

Previous studies (Ghomi and El-Salakawy 2015; Hasaballa and El-Salakawy 2015) showed that concrete beam-column joints reinforced with Glass (G) FRP are able to reach high drift ratios (up to 6%) with minor residual damage. This is expected to reduce repair cost after a seismic event. However, despite the promising results of the early programs, the number of studies in this area is still very few.

Due to this lack of research and data, current codes and guidelines for FRP-RC structures do not have comprehensive provisions for seismic design. For example, although the CSA S806-12 (CSA 2012), in Chapter 12, provides the amount of transverse reinforcement required to confine an FRP-RC column subjected to seismic loading, it does not indicates the shear capacity of beam-column joints constructed according to this provision. Ghomi and El-Salakawy (2015) and Hasaballa and El-Salakawy (2015)

investigated the shear capacity of various configurations of exterior GFRP-RC beam-column joints; however, there are still many parameters, which are known to affect the seismic performance of FRP-RC beam-column joints, are not investigated.

In this program, a series of finite element models were built using a specialized software (ATENA ver. 5) to simulate seismic behaviour of GFRP-RC exterior beam-column joints previously tested by the authors (Ghomi and El-Salakawy 2015) and to perform an analytical study on possible affecting parameters.

2. Summary of Experimental Program

2.1. Test specimens

As part of the study conducted by the authors (Ghomi and El-Salakawy 2015), two full-scale exterior GFRP-RC beam-column joints with lateral beams were constructed and tested under reversal cyclic loading. The specimens were extracted from an arbitrary RC moment-resisting frame at assumed points of contra-flexure, at mid-height of columns and mid-span of beams. Figure 1.a shows dimensions of the specimens. The specimens were identical except for the number of beam longitudinal reinforcement bars, which resulted in different shear stress applied to the joint, $0.8\sqrt{f'_c}$ and $1.1\sqrt{f'_c}$. In this program, the specimens were named E-0.8 and E-1.1, respectively. Table 1 shows specimens properties.

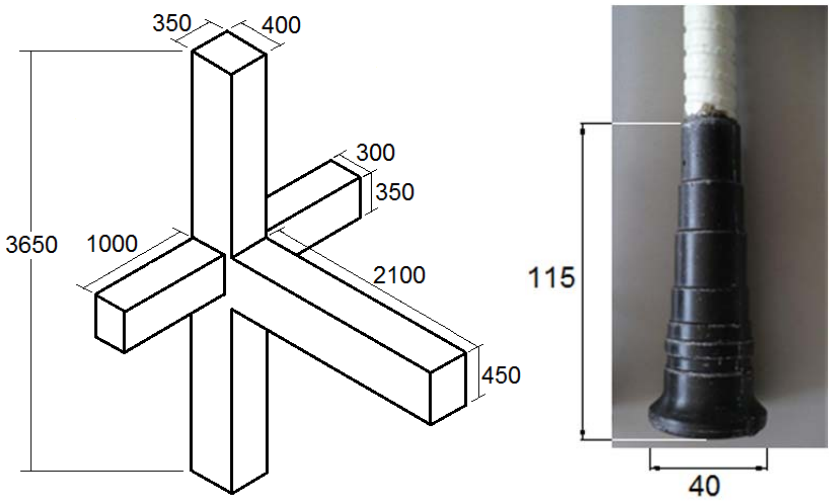

(a) Specimens dimensions (mm) (b) Beam longitudinal bars anchorage

Figure 1 – Specimens dimension and bars anchorage type

The specimens were cast with normal-weight ready-mix concrete with maximum aggregate size of 20 mm and target strength of 35 MPa. Ribbed-deformed GFRP bars and stirrups (Schoeck Canada Inc. 2012) were used to reinforce the specimens. Table 2 gives the properties of the used GFRP reinforcement, obtained by CSA S806-12 (CSA 2012) standard tests. It should be mentioned that mechanical anchorage (headed-end bars) was used to anchored beam longitudinal bars inside the joint (Figure 1.b).

2.2. Test set-up and loading procedure

Figure 2 shows the test set-up. The specimens were rotated 90-degree to facilitate the testing procedure. The columns were in horizontal position and subjected to constant axial load during the test. The axial load was equal to approximately 15% of the columns maximum concentric capacity. Also, during testing, lateral beams were under a constant load, equal to service load, in order to include the effect of out-of-plane moments on the behaviour of the joint.

A quasi-static reversal cyclic load, based on ACI 374.1-05 (ACI 2005), was applied to the tip of the beam by means of a 1000-kN capacity actuator. The displacement-controlled cyclic loading was applied in several loading steps, gradually increasing in lateral drift ratio. It should be mentioned that drift ratio is defined as the ratio of beam tip displacement over the beam length. Each loading step consists of three identical loading cycles to ensure stable crack propagation. After 2% drift ratio stage, one load-controlled cycle with a peak load equal to service condition was applied after each loading step. The service loading

condition is defined as the load corresponding to 25% of the ultimate strain of GFRP beam longitudinal bars. Figure 3 shows loading scheme.

Table 1: Design characteristics of tested specimens

Specimen ID	ρ / ρ_{bal} *	Beam Flexural Capacity (kN.m)	Flexural Strength Ratio	Joint shear Stress (MPa)	Concrete Strength (MPa)
E-0.8	1.64	307	1.61	$0.81\sqrt{f'_c}$	44
E-1.1	3.62	365	1.35	$1.1\sqrt{f'_c}$	42

* ρ / ρ_{bal} is the ratio between the provided reinforcement ratio to the balanced reinforcement ratio of the beam section.

Table 2: Properties of GFRP bars (at the straight portion of the bars)

Bar configuration	Bar Diameter (mm)	Tensile Elastic Modulus (GPa)	Ultimate Tensile Strength (MPa)	Ultimate Tensile Strain (%)
Stirrups	12	50	750	1.50
Headed Bars	16	60	1100	1.83

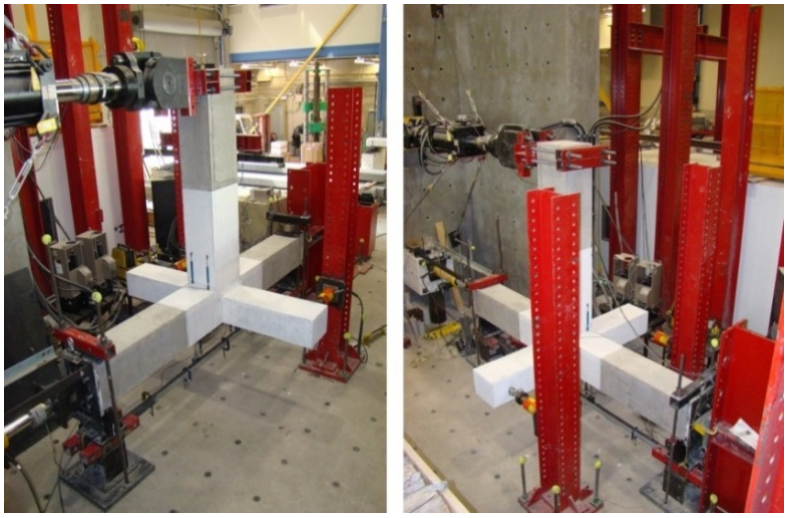

Figure 2 – Test set-up

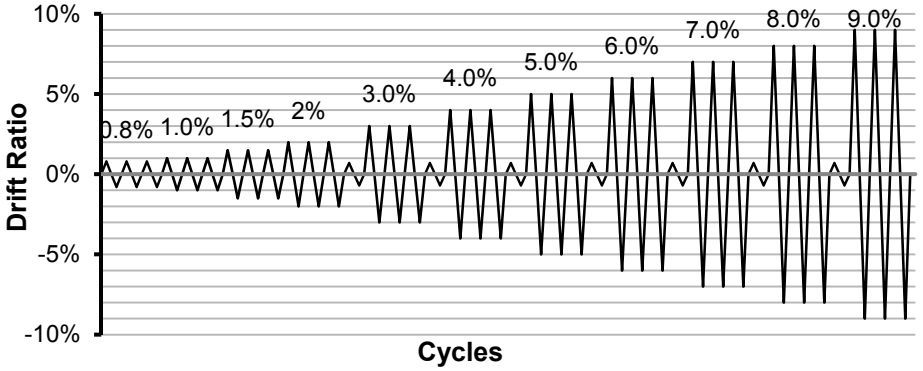

Figure 3 – Loading scheme

2.3. Hysteresis diagram

Figure 4 shows lateral load-drift response of the tested specimens. Both specimens showed similar linear behaviour up to 6% drift ratio. However, the magnitude of joint shear stress significantly influenced the behaviour of the specimens after 6% drift ratio. Specimen E-0.8 exhibited brittle failure at 7% drift ratio due to rupture of beam longitudinal bars, while Specimen E-1.1 exhibited nonlinear response after 6% drift ratio despite the expected linear behaviour of FRP-RC elements. The specimen maintained its lateral load carrying capacity up to 8% drift ratio. The test was stopped after 9% drift ratio due to a significant decrease in the specimen's load carrying capacity (more than 40%). The dashed lines in the figures refer to design capacity of the specimens based on concrete strength on the day of testing. Both specimens reached their design capacity at 4% drift ratio.

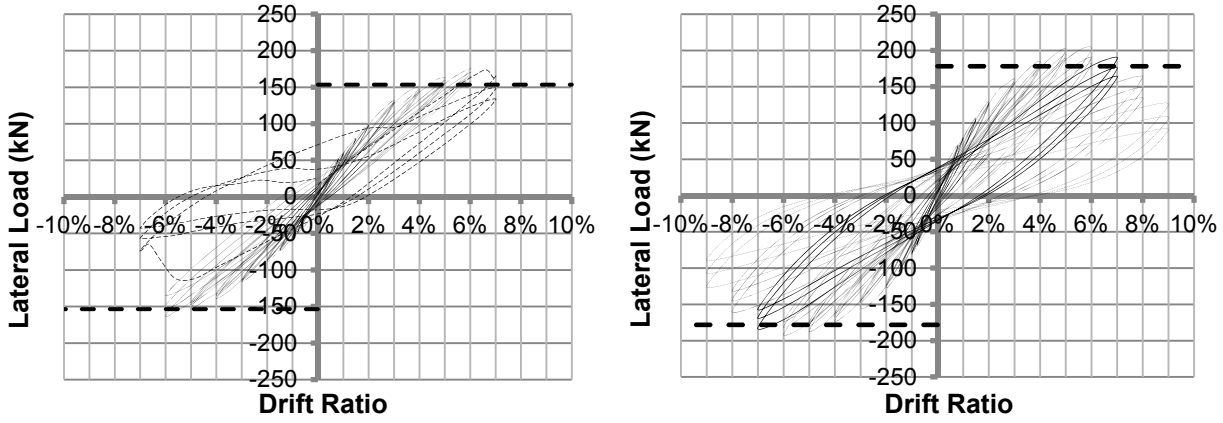

(a) Specimen E-0.8 (b) Specimen E-1.1

Figure 4 – Lateral load-drift response of test specimens

2.4. Mode of failure

Figure 5 shows pictures of the specimens at failure. The majority of the damage in Specimen E-0.8 was concentrated in the beam while the joint remained intact. Specimens E-1.1, on the other hand, exhibited significant damage in the joint area due to high joint shear stress.

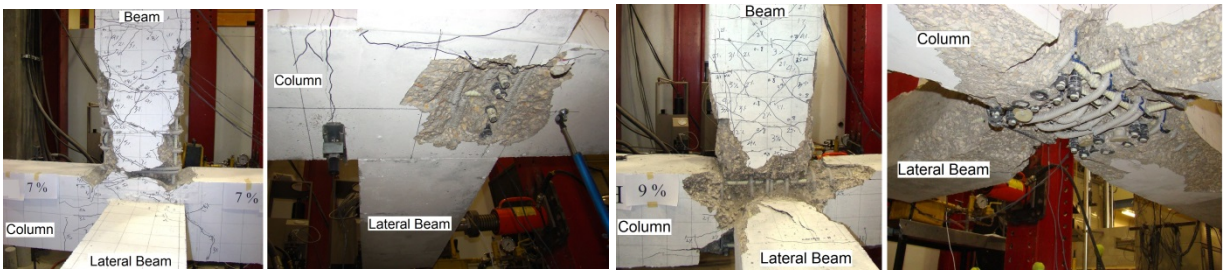

(a) Specimen E-0.8 (b) Specimen E-1.1

Figure 5 – Picture of test specimens at failure

It should be mentioned that despite the different mode of failure of the specimens, both specimens not only achieved their design capacity but also exceeded that limit. Moreover, lateral drift capacity of the specimens (7% and 9% for E-0.8 and E-1.1, respectively) was significantly higher than the maximum lateral drift expected from a reasonably designed frame. The National Building Code of Canada (NRCC 2010) limits lateral drift of stories to 2.5% to eliminate possibility of structural failure due to excessive P-Δ moments. In addition, the maximum expected lateral drift ratio of a story in CSA/S806-12 (CSA 2012) is 4%. Therefore, although the behaviour of beam-column joints at high drift ratios is of academic interest, it may not be applicable in real structures. Therefore, a threshold of 4% is set in evaluating the performance of simulated beam-column joints.

Figure 6 shows pictures of the test specimens after 4% drift ratio-loading step. According to the pictures, the damage is limited to the beam concrete cover and there is no signs of significant damage in the joint. This is in good agreement with the hysteresis diagram of the specimens with narrow loops and insignificant residual displacement at zero load.

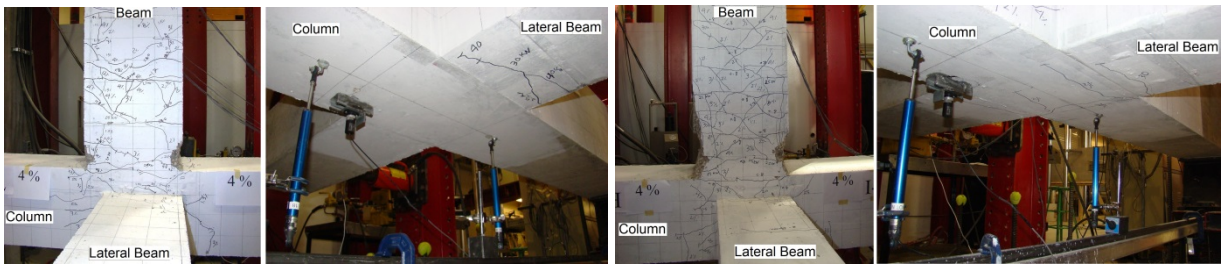

(a) Specimen E-0.8 (b) Specimen E-1.1

Figure 6 – Picture of test specimens after 4% drift ratio

3. Finite Element Modelling

In order to further investigate key parameters affecting the seismic performance of FRP-RC beam-column joints, a finite element model (FEM) was built to simulate the behaviour of RC beam-column joints under reversal loading. The specialized finite-element software ATENA-3D (version 4.3.1) was used to build the models.

3.1. Concrete material

Eight-node brick elements, "CCIsoBrick", were used in modeling concrete geometry. To model concrete material, Fracture-Plastic Constitutive Model (CC3D Non-Linear Cementitious 2) was used. In this model, ATENA-3D combines two different constitutive models for tensile (fracture) and compressive (plastic) behaviour of concrete. The classical orthotropic smeared crack formulation and crack band model is used for fracture model. This model employs Rankine failure criterion and exponential softening. For compressive behaviour of concrete, the program uses a softening/hardening plasticity model based on Menétrey-Willam failure surface. The model adopts elliptical hardening and linear softening relationship based on the experimental work of Van Mier (1986). This model can be used to simulate concrete cracking and crushing under high confinement.

Based on research work of Vecchio and Collins (1986), compressive strength of concrete is decreased when cracking occurs in the perpendicular direction. In ATENA-3D, this compressive strength reduction is limited by a coefficient, $r_{c,lim}$, which in this study was taken as 0.9. Moreover, the effect of cracked concrete on tensile stiffness of reinforcements (tension stiffening) is accounted for in ATENA-3D. The program specifies a tension-stiffening factor, c_{ts}, which represents a relative limiting value of tensile strength in the tension-softening of concrete. This value was set as 0.4 in this study. More details on material modeling in ATENA-3D can be found in the user manual of the software (*Cervenka et al.* 2012).

3.2. Reinforcement material

In this study, a discrete model was used for both longitudinal and transverse reinforcement. The GFRP material was modeled with a linear behaviour having a maximum tensile strength and strain of 1100 MPa and 1.83%, respectively. ATENA-3D provides the option of defining bond-slip relationship between reinforcing bars and surrounding concrete. The bond-slip relationship, provided by the manufacturer, for ribbed-deformed GFRP bars (Figure 7) was used to simulate the behaviour of GFRP-RC beam-column joints under seismic loading.

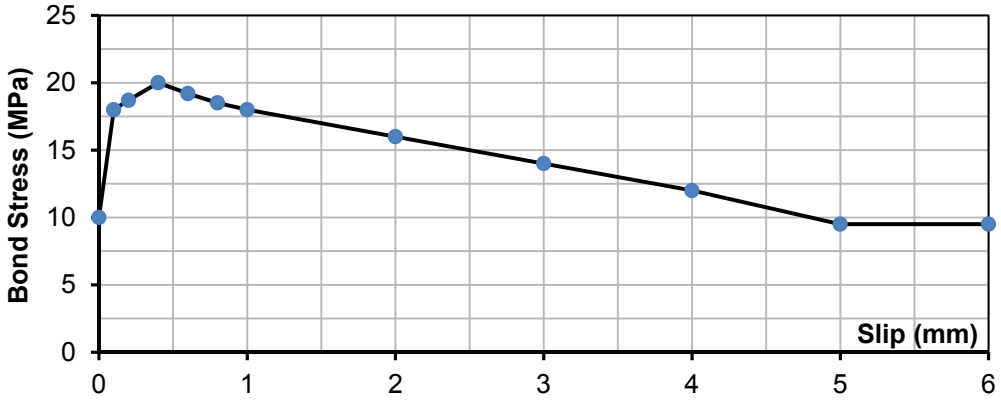

Figure 7 – Bond-slip relationship of GFRP bars and concrete

3.3. Model verification and parametric study

In order to verify the constructed FEM, the results of the model were compared with results of the test specimens. Figure 8 compares lateral load-drift response of the tested and modeled specimens in the first cycle of loading in each loading step up to 4% drift ratio. According to the figure, results are in reasonable agreement.

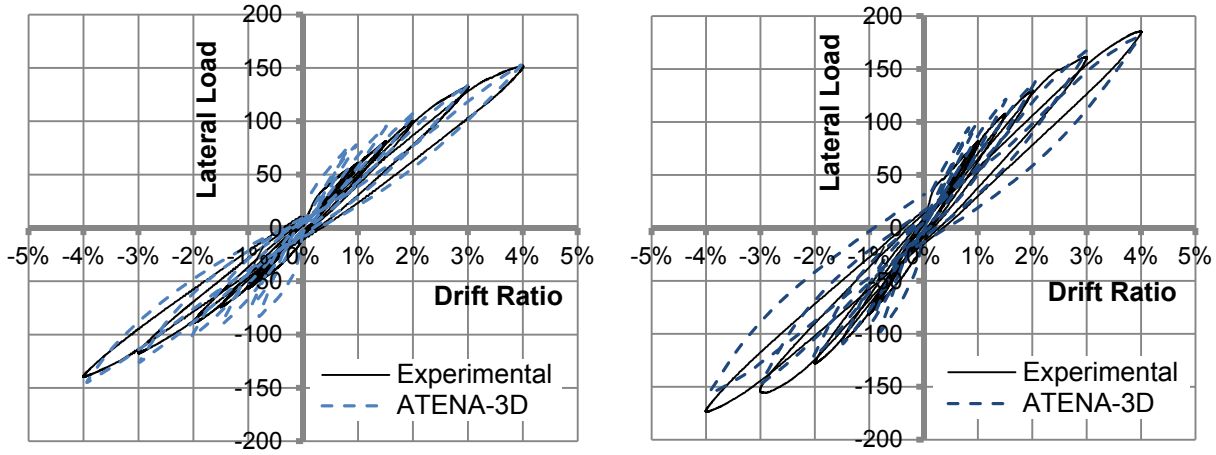

(a) Specimen E-0.8 (b) Specimen E-1.1

Figure 8 – Hysteresis diagrams of test specimens and corresponding modeled specimens

The verified FEM was used to study the effect of three parameters on the seismic behaviour of GFRP-RC exterior beam-column joints: 1) joint shear stress, 2) presence of lateral beams and 3) concrete strength. Table 3 shows properties of the simulated specimens.

4. Results and Discussion of FEM

4.1. Joint shear stress

Since Specimen E-1.1 was able to reach its design capacity without any significant damage at the joint area, it was concluded that GFRP-RC exterior beam-column joints with lateral beams can withstand joint shear stress of $1.1\sqrt{f'_c}$. However, yet it is not clear that whether such joints can withstand higher joint shear ratios or not. In order to answer this question, a beam-column joint, identical to Specimen E-1.1 except for the beam longitudinal bars diameter (or area), was simulated with ATENA-3D (Specimen A-1.3). In this model, beam longitudinal bars diameter was increased to 20 mm, which resulted in joint shear stress of $1.3\sqrt{f'_c}$.

Figure 9 shows lateral load-drift response of A-1.3. According to the graphs, the specimen showed linear behaviour without significant residual damage at zero-load condition up to 2% drift ratio. However,

excessive concrete damage at the joint, due to high joint shear stress, significantly decreased the stiffness of the specimen and resulted in wide hysteresis loops for drift ratios greater than 2%. The specimen was not able to achieve its design capacity indicating that $1.3\sqrt{f'_c}$ is more than shear capacity of GFRP-RC exterior beam-column joints with lateral beams.

Table 3: Analytical test matrix

Study Parameter	Specimen ID	Lateral Beams	Joint Shear Stress × $\sqrt{f'_c}$	Concrete Compressive Strength (MPa)
Joint Shear Stress	A-1.3	Yes	1.3	42
Presence of Lateral Beams	A-0.8-N	No	0.8	44
	A-1.1-N	No	1.1	42
Concrete Compressive Strength	A-30	Yes	1.1	30
	A-40	Yes	1.1	40
	A-50	Yes	1.1	50
	A-60	Yes	1.1	60
	A-70	Yes	1.1	70
	A-80	Yes	1.1	80

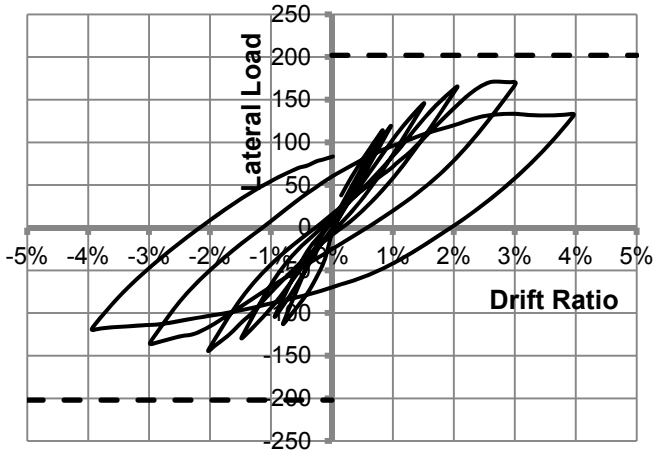

Figure 9 – Hysteresis diagram of Specimen A1.3

4.2. Effect of lateral beams

Two FEMs were constructed to simulate specimens E-0.8 and E-1.1 without lateral beams to investigate influence of the confinement provided by lateral beams on shear capacity of exterior beam-column joints. Figure 10 compares envelop of hysteresis diagrams of the tested specimens with their corresponding FEMs without lateral beams.

According to the graphs, Specimen A-0.8-N showed very similar behaviour to Specimen E-0.8. The low joint shear stress in A-0.8-N resulted in insignificant concrete damage and expansion at the joint area up to 4% drift ratio. Therefore, additional confinement provided by lateral beams in E-0.8 did not affect the behaviour of the specimen. In Specimen A-1.1-N, on the other hand, high joint shear stress caused significant concrete damage and expansion in the joint area, which prevented the specimen from achieving its design capacity. In this case, adding additional confinement to the joint by means of lateral beams limited concrete expansion and contributed to maintain the joint's integrity. Therefore, the seismic

behaviour of E-1.1 showed significant improvement and the specimen reached its design capacity without significant damage in the joint area.

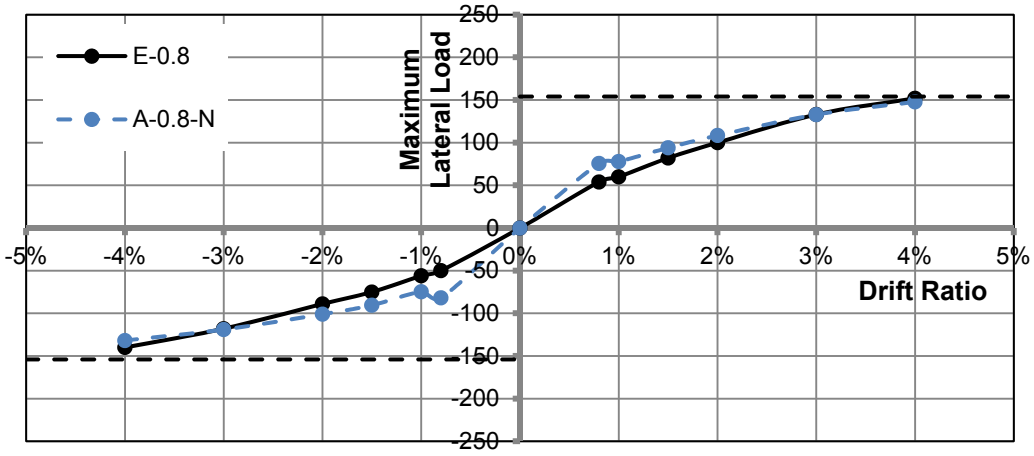

(a) Specimens E-0.8 and A-0.8-N

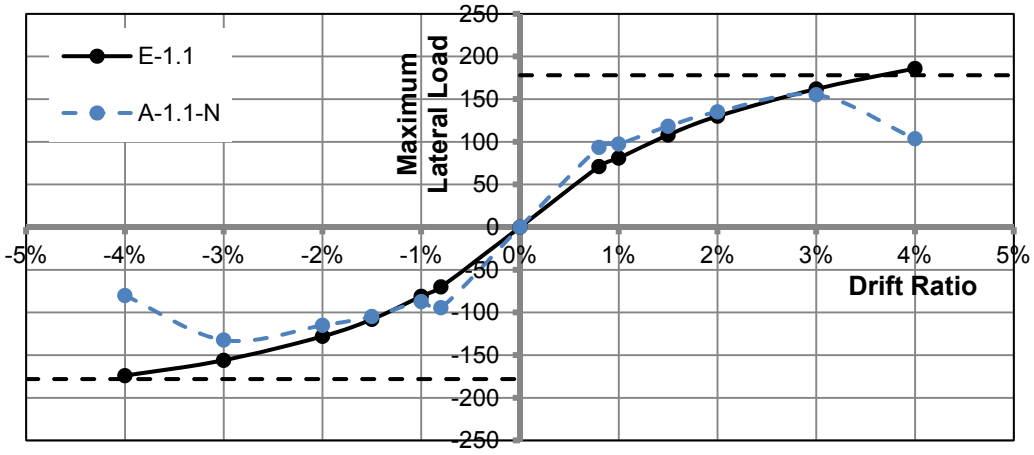

(b) Specimens E-1.1 and A-1.1-N

Figure 10 – Envelops of test specimens and corresponding modeled specimens without lateral beams

4.3. Effect of concrete compressive strength

In order to investigate the effect of concrete compressive strength on the seismic performance of beam-column joints, the FEM of Specimen E-1.1 was run with various concrete strengths, ranging from 30 to 80 MPa with 10 MPa increments. Figure 11 shows the hysteresis diagram envelops of the simulated models.

According to the graph, the concrete compressive strength is in inversely related to the percentage of the design load achieved at 4% drift ratio. In other words, although higher concrete strength increases the design capacity, it also increases the drift ratio that the specimen achieves its design capacity at. As shown in the graph, Specimen A-30 reached it's design capacity at 3% drift ratio, while Specimen A-80 was able to reach only 90% of its design capacity at 4% drift ratio. It worth reapeting that the simulation was stoped after 4% drift ratio and none of the specimens failed till that level.

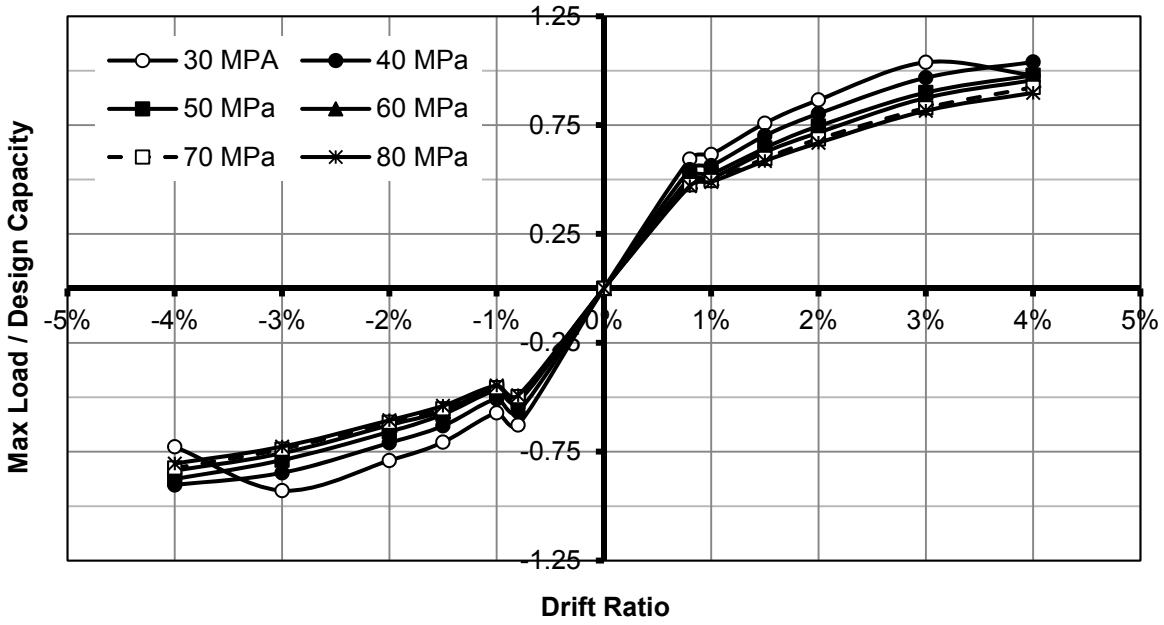

Figure 11 – Hysteresis diagrams for concrete strength parameter

5. Conclusions

Based on the results obtained from experimentally tested and FEM simulated specimens, the following conclusions can be made:

1. The GFRP-RC exterior beam-column joint confined with lateral beams and joint shear stress of $1.1\sqrt{f'_c}$ (Specimen E-1.1) was able to reach its design capacity at 4% drift ratio without significant damage in the joint area. However, increasing the joint shear stress to $1.3\sqrt{f'_c}$ resulted in premature failure of Specimen A-1.3, due to excessive damage induced to the joint. Therefore, it can be concluded that $1.3\sqrt{f'_c}$ is beyond the shear capacity of such joints.
2. The effect of lateral beams on seismic performance of GFRP-RC beam-column joints is related to the level of joint shear stress. In Specimen A-0.8-N, due to low joint shear stress ($0.8\sqrt{f'_c}$), insignificant concrete expansion occurred in the joint area. Therefore, additional confinement provided by lateral beams did not play significant role in improving shear capacity of the joint. However, in Specimen A-1.1-N with higher joint shear stress ($1.1\sqrt{f'_c}$) the confinement provided by lateral beams significantly improved seismic performance of the joint by preventing joint's concrete expansion.
3. Concrete compressive strength significantly influences the drift ratio that a GFRP-RC exterior beam-column joint achieves its design capacity at. Specimen A-30 with concrete compressive strength of 30 MPa and joint shear stress of $1.1\sqrt{f'_c}$ reached its design capacity at 3% drift ratio, while Specimen A-80 with the same joint shear stress and concrete strength of 80 MPa was able to reach only 90% of its design capacity at 4% drift ratio.

6. Acknowledgements

The authors wish to express their gratitude for the financial support received from the Natural Science and Engineering Research Council of Canada (NSERC), through Discovery and Canada Research Chairs program. The GFRP reinforcement was generously provided by Schoeck Canada Inc.

7. References

American Concrete Institute (ACI) Committee 374, "Acceptance criteria for moment frames based on structural testing and commentary." ACI 374.1-05, Farmington Hills, Mich, 2005.

Cervenka, V., Jendele, L., Cervenka, J., “ATENA Program Documentation Part 1: Theory.” Cervenka Consulting Ltd., Prague, Czech Republic, 2012.

Canadian Standards Association (CSA), “Design and construction of building components with fibre reinforced polymers.” CAN/CSA-S806-12, Ontario, Canada, 2012.

Fukuyama, H., Masuda, Y., Sonobe, Y. and Tanigaki, M, “Structural Performances of Concrete Frame Reinforced with FRP Reinforcement.” *Proceeding of the 2nd international RILEM Symposium, Non-Metallic (FRP) Reinforcement for Concrete Structures*, 1995, pp. 275-286.

Ghomi, S. and El-Salakawy, E., “Seismic Performance of GFRP-RC Exterior Beam-Column Joints with Lateral Beams.” *Journal of Composites for Construction*, ASCE, published on-line on April 2015.

Hasaballa, M.H. and El-Salakawy, E., “Shear Capacity of Type-2 Exterior Beam-Column Joints Reinforced with GFRP Bars and Stirrups.” *Journal of Composites for Construction*, ASCE, published on-line on April 2015.

Mady, M., El-Ragaby, A. and El-Salakawy, E., “Seismic Behavior of Beam-Column Joints Reinforced with GFRP Bars and Stirrups.” *Journal of Composites for Construction*, ASCE, 2011, Vol. 15, No. 1, pp 875-886.

National Research Council of Canada (NRCC), "National Building Code of Canada (NBCC)." Ottawa, Ontario, 1245 p, 2010.

Said, A.M., Nehdi, M.L., “Use of FRP for RC Frames in Seismic Zones: Part II. Performance of Steel-Free GFRP-Reinforced Beam-Column Joints.” *Applied Composite Materials*, 2004, Vol. 11, No. 4, pp 227-245.

Schoeck Canada Inc., Schöck-ComBAR™, *Technical Information sheet*, Available from http://www.schoeck-canada.com/en_ca/download/combar--17#

Vecchio, F. and Collins, M., “The modified compression-field theory for reinforced concrete elements subjected to shear.” *ACI Journal*, 1986, Vol. 83, No. 2, pp 219-231.